JACS
JOURNAL OF THE AMERICAN CHEMICAL SOCIETY
pubs.acs.org/JACS
Article

Molecular Recognition and Cocrystallization of Methylated and Halogenated Fragments of Danicalipin A by Enantiopure Alleno-Acetylenic Cage Receptors

Cornelius Gropp, Stefan Fischer, Tamara Husch, Nils Trapp, Erick M. Carreira,* and François Diederich*

Cite This: https://dx.doi.org/10.1021/jacs.9b13217

Read Online

ACCESS | Metrics & More | Article Recommendations | Supporting Information

ABSTRACT: Enantiopure $(P)_4$- and $(M)_4$-configured alleno-acetylenic cage (AAC) receptors offer a highly defined interior for the complexation and structure elucidation of small molecule fragments of the stereochemically complex chlorosulfolipid danicalipin A. Solution (NMR), solid state (X-ray), and theoretical investigations of the formed host–guest complexes provide insight into the conformational preferences of 14 achiral and chiral derivatives of the danicalipin A chlorohydrin core in a confined, mostly hydrophobic environment, extending previously reported studies in polar solvents. The conserved binding mode of the guests permits deciphering the effect of functional group replacements on Gibbs binding energies ΔG. A strong contribution of conformational energies toward the binding affinities is revealed, which explains why the denser packing of larger apolar domains of the guests does not necessarily lead to higher association. Enantioselective binding of chiral guests, with energetic differences $\Delta\Delta G_{293\ K}$ up to 0.7 kcal mol^{-1} between diastereoisomeric complexes, is explained by hydrogen- and halogen-bonding, as well as dispersion interactions. Calorimetric studies (ITC) show that the stronger binding of one enantiomer is accompanied by an increased gain in enthalpy ΔH but at the cost of a larger entropic penalty $T\Delta S$ stemming from tighter binding.

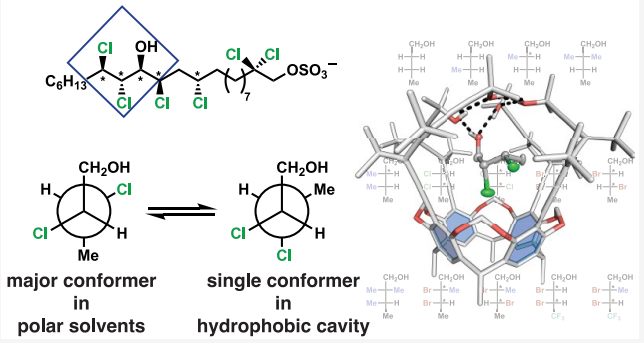

INTRODUCTION

The complexation and crystallization of small molecules in the interior of receptor systems not only allow structure elucidation of target molecules with atomic resolution but also enable the study of intermolecular interactions and conformational preferences of guests in confined chemical space.[1]

In our previous studies, we identified enantiopure alleno-acetylenic cage (AAC) receptors $(P)_4$- and $(M)_4$-**1** as privileged receptor systems to investigate the molecular recognition and cocrystallization of small molecules—cyclo-alkanes and tropane derivatives—containing both polar and apolar functionalities (Figure 1A).[2] The tertiary hydroxy groups of the homochiral alleno-acetylenic arms of the receptor establish a 4-fold hydrogen-bonding array in the closed cage conformation.[2a,3] Upon encapsulation of short-chain alcohols, the 4-fold H-bonding array of the host is expanded to incorporate the hydroxy group of the guest in pentagonal and 4-fold and docking as well as hexagonal H-bonding networks that close the cage.[4] The lean, all-carbon acetylenic backbone of the receptor forms a highly confined, rather lipophilic cavity that facilitates dispersion and halogen-bonding interactions with apolar domains of the guest.[5] These structural attributes of the interior of the receptor resemble the characteristic hydrophilic and hydrophobic domains of lipid structures.[2b]

Chlorosulfolipids are a class of marine membrane lipids that have drawn wide attention from a synthetic perspective because of the complex stereochemistry originating from their polychlorinated backbone.[6] Although little is known about their biological activity, cell-based studies have demonstrated their ability to compromise cell membranes, presumably as a result of their discrete conformation adopted in the lipophilic environment of the membrane.[7] NMR spectroscopic studies on chlorohydrin fragments of these natural products have allowed detailed analysis of their conformation and configuration in polar solvents.[8] However, scarce solubility of the chlorosulfolipids in apolar solvents has

Received: December 8, 2019

https://dx.doi.org/10.1021/jacs.9b13217
J. Am. Chem. Soc. XXXX, XXX, XXX−XXX

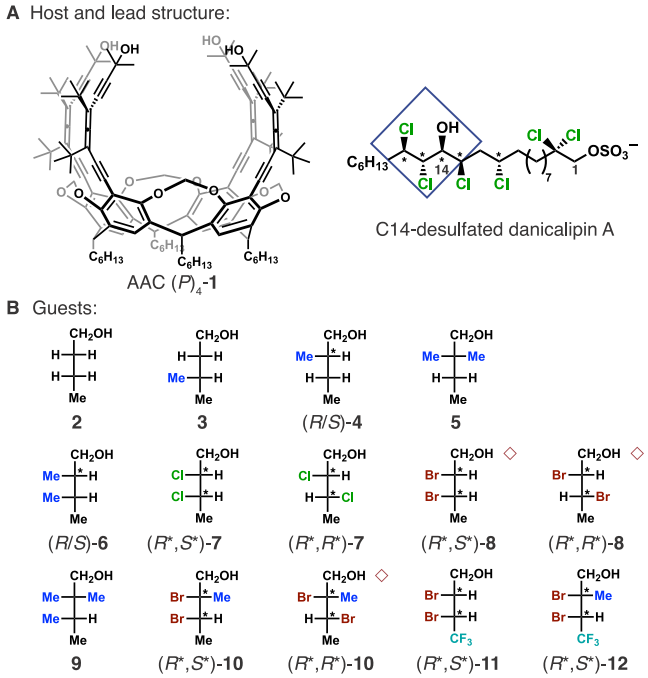

Figure 1. A) $(P)_4$-configured alleno-acetylenic cage (AAC) receptor **1** and C14-desulfated danicalipin A as lead structure. B) Summary of guest molecules **2**–**12**; structures are shown as racemates in the Fischer projection. Starred C atoms are stereogenic centers; chiral guests were synthesized as racemates. Structures designated with a red diamond were separated into their enantiomers.

prevented their conformational analysis in a more hydrophobic environment.

Alleno-acetylenic cage receptors, $(P)_4$- and $(M)_4$-**1**, offer a well-defined, mostly lipophilic environment for the complexation and conformational analysis of lipid fragments, together with a fast readout both in solution by nuclear magnetic resonance (NMR) and electronic circular dichroism (ECD) spectroscopy as well as isothermal titration calorimetry (ITC) and in the solid state by X-ray cocrystal structure analysis. Complexation studies of chlorohydrin fragments with our AAC model system give insight into the adopted conformation of small molecule fragments of chlorosulfolipids in a more hydrophobic environment (for isosurface calculations on the host, see ref 2b).

Isosteric replacements of the functional groups, a widely used strategy to optimize the biological activity of lead candidates, allow for studying the contribution of dispersion interactions, halogen-bonding, and dense packing to their binding affinities.[9,10] We present a series of 14 target molecules with up to two stereogenic centers (Figure 1B). Of particular interest is the effect of the functional group replacements on the binding affinities and preferred conformations of the complexed guests.

METHODOLOGY

The chiral guest molecules were synthesized as racemates (see Supporting Information, Experimental Section S2). Structures designated with a red diamond in Figure 1B were separated into their respective enantiomers. The binding affinities of the guests toward the enantiopure receptors were quantified in solution through ECD spectroscopy and ITC.[11] The solution-state host–guest complexes were characterized by 1D and 2D NMR spectroscopic studies. *n*-Octane was chosen as a weakly competitive solvent for both techniques. Single crystal X-ray

A: ITC & ECD Spectroscopy

$(P)_4$-**1**⊃ Guest	K_a (ITC)/ [M^{-1}]	K_a (ECD)/ [M^{-1}]	$\Delta G_{293\,K}$ (ITC)/ [kcal mol^{-1}]	$\Delta G_{293\,K}$ (ECD)/ [kcal mol^{-1}]
2	–	–	<1	<1
3	$1.6\cdot10^3$	$1.5\cdot10^3$	–4.3	–4.3
(*R*/*S*)-**4**	$4.6\cdot10^3$	$2.3\cdot10^3$	–4.9	–4.5
5	$2.0\cdot10^4$	$1.7\cdot10^4$	–5.8	–5.7
(*R*/*S*)-**6**	$9.9\cdot10^3$	$5.9\cdot10^3$	–5.4	–5.1
(*R**,*S**)-**7**	$1.1\cdot10^4$	$1.8\cdot10^4$	–5.4	–5.7
(*R**,*R**)-**7**	$9.0\cdot10^4$	$7.0\cdot10^4$	–6.6	–6.5
(*R**,*S**)-**8**	$6.6\cdot10^4$	$7.6\cdot10^4$	–6.5	–6.5
(*R**,*R**)-**8**	$4.8\cdot10^5$	$3.8\cdot10^5$	–7.6	–7.5
9	$6.9\cdot10^3$	$8.2\cdot10^3$	–5.1	–5.2
(*R**,*S**)-**10**	$1.4\cdot10^5$	$1.2\cdot10^5$	–6.9	–6.8
(*R**,*R**)-**10**	$3.8\cdot10^5$	$7.4\cdot10^5$	–7.5	–7.9
(*R**,*S**)-**11**	$1.7\cdot10^4$	$1.3\cdot10^4$	–5.7	–5.5
(*R**,*S**)-**12**	$1.8\cdot10^4$	$1.2\cdot10^4$	–5.7	–5.5

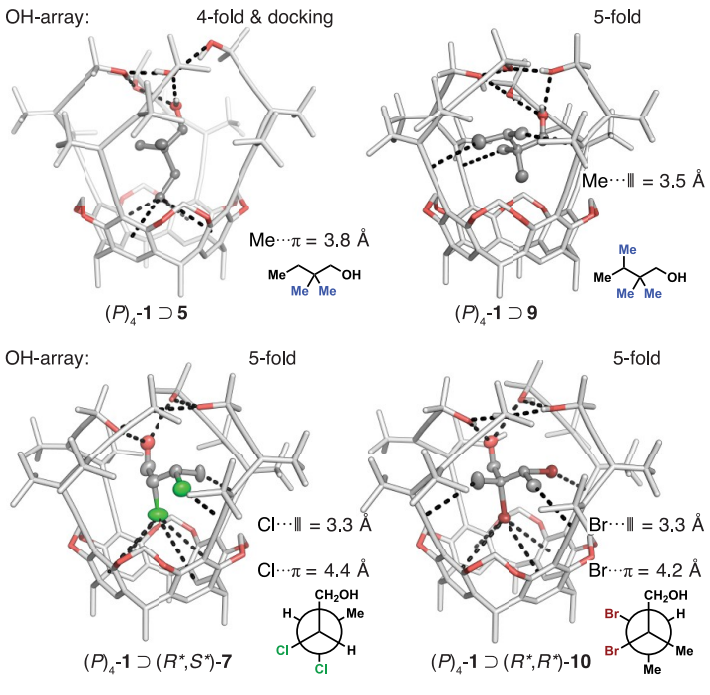

Figure 2. A) Binding constants (K_a) by ECD spectroscopic and ITC titrations with AAC $(P)_4$-**1** and guests **2**–**12** in *n*-octane at 293 K; for details, see Supporting Information, Sections S3–S7. The overall error in K_a is estimated to be ±20% ($\Delta G_{293\,K}$ ± 0.2 kcal mol^{-1}). B) Single crystal X-ray cocrystal structures of AAC $(P)_4$-**1** with guests **5**, **9**, (*R**,*S**)-**7**, and (*R**,*R**)-**10**; only one enantiomer of the guest is shown. CCDC numbers: 1914838; 1914840; 1914858; 1914842. The nature of the expanded H-bonding networks closing the cages is indicated. Corresponding X-ray cocrystal structures with $(M)_4$-**1** are shown in the Supporting Information, Section S11.

https://dx.doi.org/10.1021/jacs.9b13217
J. Am. Chem. Soc. XXXX, XXX, XXX–XXX

structures of 14 host−guest complexes give insight into the binding mode and the adopted conformation of the complexed guests in the solid state.[12] Details are provided in the Experimental Section of the Supporting Information (S1−S12).

Packing coefficients of the host−guest complexes were calculated based on the obtained X-ray cocrystal structures and are provided in Section S4 of the Theoretical Section of the Supporting Information.

All guest structures were optimized with the Perdew−Burke−Ernzerhof density functional (PBE)[13] in combination with empirical D3 dispersion corrections (PBE-D3).[14] We chose a def2-TZVPP basis set[15] for the PBE-D3 calculations. Details on the theoretical methodology are provided in the Theoretical Section of the Supporting Information (S1−S3).

RESULTS AND DISCUSSION

Our initial focus was to study the influence of the degree of methyl substitution of the unfunctionalized *n*-butanol core (**2**−**6**, **9**) of danicalipin A on the binding affinity to the host (additional methyl groups are highlighted in blue, Figure 1B), exploring whether denser packing and optimized dispersion interactions lead to an increase in association strength.[9]

While unfunctionalized *n*-butanol **2** did not show quantifiable association with the receptor, the introduction of a single methyl group to the backbone, such as in primary alcohols **3** and (*R*/*S*)-**4**, induced a large increase in binding affinities to $\Delta G_{293\ K} = -4.3$ and -4.8 kcal mol^{-1}, respectively (Figure 2A). The addition of a second methyl group in positions 2 or 3 of the *n*-butanol chain only slightly enhanced the binding strength by $\Delta\Delta G_{293\ K} = -0.6$ and -1.0 kcal mol^{-1} (guests **5** and (*R*/*S*)-**6**, Figure 2A). 2,2,3-Trimethylbutan-1-ol **9**, decorated with three methyl groups, did not show further increase in association strength but bound with comparable binding affinity to guests **3** and (*R*/*S*)-**4** ($\Delta G_{293\ K} = -5.1$ kcal mol^{-1}). The strong initial rise in binding strength with placement of one methyl group is remarkable, considering the smaller influence of additional methyl groups toward the association energies, despite denser packing of the ensemble (see Section S4 of the Theoretical Section of the Supporting Information).[9]

The X-ray cocrystal structures of AAC $(P)_4$-**1** with molecules **5** and **9** show two different binding modes of the aliphatic alcohols in the interior of the host (Figure 2B). 2,2-Dimethylbutan-1-ol **5** is engaged in a 4-fold and docking topology with the host, with the terminal methyl group pointing toward the aromatic resorcin[4]arene core of the receptor (average C−H···π distances of 3.8 Å).[16] In this binding mode, the terminal methyl group is *anti-periplanar* relative to the CH_2OH-functionality (Figure 3A). In contrast, 2,2,3-trimethylbutan-1-ol **9** forms a puckered pentagonal 5-fold H-bonding network with the host (Figure 2B). The two terminal methyl groups point toward the acetylenic functionality rather than the aromatic core (C−H···||| distances of 3.5−3.8 Å), adopting an *anti-periplanar* and a *gauche* conformation relative to the CH_2OH group (Figure 3B). The increased packing density and optimized dispersion interactions of guest **9** compared to guest **5** are presumably compensated by the conformational energy resulting from the additional methyl group, which explains the overall decrease in binding affinity despite denser packing (Figure S131 of the Supporting Information). Remarkably, the achiral guest **9** is complexed in two chiral conformations, which are enantiomers of each other. The higher occupancy of one conformational enantiomer (60:40 for $(P)_4$-**1** and 42:58 for $(M)_4$-**1**, Figure 3B) indicates the preferential binding of one conformational enantiomer over the other and exemplifies the highly asymmetric environment of the cavity.[17]

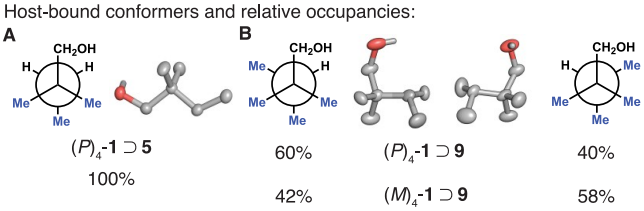

Figure 3. Host-bound conformations extracted from the X-ray cocrystal structures of AAC $(P)_4$-**1** with guest **5** (A) and of AACs $(P)_4$-**1** and $(M)_4$-**1** with **9** (B). Relative occupancies of the enantiomeric conformations of guest **9** complexed to $(P)_4$- and $(M)_4$-**1** are shown. CCDC numbers: 1914838; 1914840; 1914836.

Variable temperature (VT) NMR spectroscopic binding studies substantiated the binding mode of the aliphatic alcohols also in solution. At 277 K, the two singlet ^{1}H resonances corresponding to the methyl groups of the host-bound guest **9** are broad and upfield shifted to +0.19 and +0.73 ppm, respectively, compared to the free guest, indicating shielding of the methyl groups by the acetylenic moieties (see Supporting Information, Figure S49). At 238 K (Figure S50), the methyl groups of the complexed guest are shifted to +0.21 and −0.36 ppm, and the two terminal methyl groups become differentiable in the asymmetric environment of the host (two doublets at +0.21 ppm). The splitting of the ^{1}H resonances is only observed for the host-bound guest (see Supporting Information, Figures S49 and S50). In comparison, the terminal methyl group of guest (*R*/*S*)-**6** is shifted upfield (−1.9 ppm at 218 K, see Supporting Information, Figure S47), indicating close contact to the aromatic rings of the resorcin[4]arene core of the receptor and a binding mode comparable to guest **5**.[18]

The isosteric replacement of the methyl groups in (*R*/*S*)-**6** and **9** with Cl and Br leads to two diastereoisomeric sets of enantiomers, the (*R**,*S**) and (*R**,*R**) configured halohydrins, which correspond to the *anti*- and *syn*-addition products. Compared to the Me-analogues, the Cl- and Br-containing structures are able to undergo halogen-bonding interactions with the alleno-acetylenic arms of the receptor.[2b] With the halogenated fragments, we aimed to study the effects of halogen replacements of the methyl groups on the bound conformation of the guests and their influence on the binding affinities through stronger interactions.

While (*R**,*S**)-**7** showed comparable binding affinities to its Me-analog (*R*/*S*)-**6**, its diastereoisomer (*R**,*R**)-**7** gave enhanced association strength with $\Delta G_{293\ K} = -6.6$ kcal mol^{-1} ($\Delta\Delta G_{293\ K} = -1.2$ kcal mol^{-1} (*R*/*S*)-**6** → (*R**,*R**)-**7**, Figure 2A). A similar difference in binding energies between the (*R**,*S**)- and the (*R**,*R**)-diastereoisomers was also observed for bromohydrins **8**. Compound (*R**,*S**)-**8** gave binding affinities of $\Delta G_{293\ K} = -6.6$ kcal mol^{-1}, while (*R**,*R**)-**8** bound by $\Delta\Delta G_{293\ K} = -1.1$ kcal mol^{-1} stronger with $\Delta G_{293\ K} = -7.6$ kcal mol^{-1} (Figure 2A). The addition of another methyl group to the backbone to optimize shape complementary and dispersion interactions did not result in an increase in binding strength. (*R**,*S**)-**10** and (*R**,*R**)-**10** gave comparable binding affinities to the receptor as (*R**,*S**)-**8** and

https://dx.doi.org/10.1021/jacs.9b13217
J. Am. Chem. Soc. XXXX, XXX, XXX−XXX

(*R**,*R**)-**8**. This trend was already observed for the Me-isosteres in the series and can be attributed to the conformational energy resulting from the additional methyl group. The replacement of one terminal methyl group in (*R**,*S**)-**8** and (*R**,*S**)-**10** with a CF_3-group resulted in a loss of binding strength by ≈ 1 kcal mol^{-1} ($\Delta G_{293\ K}$ = −5.7 kcal mol^{-1} for (*R**,*S**)-**11** and (*R**,*S**)-**12**), indicating unfavorable interactions of the F atoms with the electron-rich aromatic rings and the alleno-acetylenes.[19]

Single crystal X-ray structures of $(P)_4$-**1**⊃(*R**,*S**)-**7** and $(P)_4$-**1**⊃(*R**,*R**)-**10** are shown as an example for the halohydrin series in Figure 2B. The crystallographic data of all complexes of $(P)_4$-**1** and $(M)_4$-**1** with halohydrin guests is given in the Supporting Information, Section S11. Structures of $(P)_4$-**1**⊃(*R**,*S**)-**7** and $(P)_4$-**1**⊃(*R**,*R**)-**10** display hydroxy groups of guests engaged in puckered pentagonal H-bonding networks with OH-groups of the receptor. The halogen atom at C2 on the *n*-butanol core points toward the acetylenic moiety, with distances of 3.2−3.3 Å (C−X···|||). The second halogen at C3 forms favorable C−X···π interactions with the host resorcin[4]arene core (average C−X···π distances of 4.2−4.4 Å). Generally, the distances between the methyl/halogen and aromatic/acetylenic counterparts decrease along the series Me → Cl → Br, consistent with some of the increase in association strength observed in solution binding studies. Noteworthy is the highly retained binding mode of guest structures **7**−**10** in the interior of the host, where all halogens are *gauche* to each other. All guests are crystallized as their racemates; the enantiomeric pairs of the guest structures generally bind in their mirror image *gauche* conformation (Figure 2B and Supporting Information, Section S11).

High retention of the binding mode of guests inside the host (for an overlay of the X-ray cocrystal structures, see the Supporting Information Figure S87) allows drawing conclusions on the contribution of functional group replacements toward their binding affinity. Figure 4 gives a summary of the differences in binding affinities of the guests toward $(P)_4$-**1** as measured by ITC.

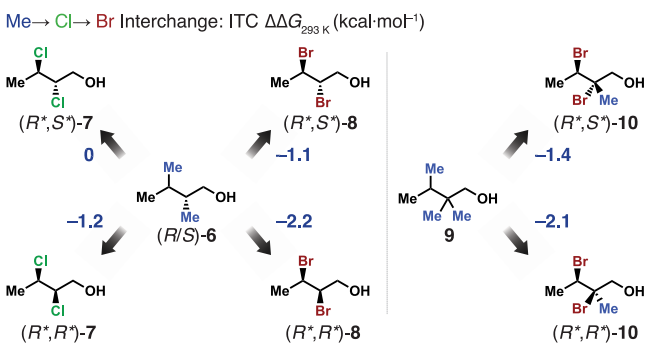

Figure 4. Schematic representation of the influence of functional group replacement in structures **6**−**10**. Differences in binding affinities are given in kcal mol^{-1} and are derived from their ITC association constants at 293 K.

Generally, binding affinities increase with establishment of halogen-bonding interactions of respective halogens with aromatic/acetylenic counterparts along the series Me → Cl → Br. It should, however, be noted that association modes of guests are not only the result of H-bonding, halogen-bonding, and dispersion interactions with interior walls of the receptor but also are influenced by the conformational energy cost of the guest necessary to adopt the host-bound conformation. The theoretically calculated conformations of the free guests in gas and condensed phases (acetonitrile) are given in the Supporting Information, Theoretical Section S1−S3. Exemplary *J*-based conformational analysis of the free guests (*R**,*S**)-, (*R**,*R**)-**7** and (*R**,*S**), (*R**,*R**)-**8** in acetonitrile is given in the Supporting Information, Section S10, Figure S77. The preferred conformations of the uncomplexed guests are compared to the host-bound conformations of the guests.

The replacement of the methyl groups in alcohol (*R*/*S*)-**6** with Cl groups does not improve binding strength for the *anti*-product (*R**,*S**)-**7**, whereas the *syn*-product yields increase in binding strength by $\Delta\Delta G_{293\ K}$ = −1.2 kcal mol^{-1}. This trend is observed in the series of guests **7**, **8**, and **10**, where *syn*-products bind by $\Delta\Delta G_{293\ K}$ ≈ 1 kcal mol^{-1} stronger compared to *anti*-products (Figure 4). This observation can be rationalized by preferred conformations of uncomplexed guest structures. Solution and theoretical studies demonstrate that uncomplexed (*R**,*S**)-configured guests **7**, **8**, and **10** preferentially adopt conformations in which the halogens are placed *anti-periplanar* to each other (Boltzmann populations based on density functional theory calculation of 0.93, 0.95, and 0.99, respectively; see also Table S41 in the Supporting Information). Upon complexation to host, guests have to undergo conformational changes from *anti-periplanar* to *gauche*. In contrast, for uncomplexed (*R**,*R**)-configured alcohols **7**, **8**, and **10**, the *gauche* conformation becomes significantly populated (Boltzmann populations of 0.65, 0.80, and 0.78, respectively). We conclude that (*R**,*S**)-configured alcohols **7**, **8**, and **10** have to undergo conformational changes upon encapsulation while (*R**,*R**)-configured alcohols do not. This is then likely reflected in generally higher association constants of *syn*-products compared to their *anti*-analogues. The results also show that replacement of Cl groups with Br groups with conserved configuration yields an increase in binding affinity of $\Delta\Delta G_{293\ K}$ ≈ 1 kcal mol^{-1}, demonstrating more effective halogen-bonding interactions of the higher halides (Figure 4).[20] Interestingly, the additional Me group at C2, such as in structures (*R**,*S**)-**10** and (*R**,*R**)-**10**, does not lead to enhanced binding, despite denser packing of guests in the interior of the host.[9,21]

The increase in binding strength upon the introduction of halogens, thereby establishing directional halogen-bonding interactions and reducing conformational costs for binding, is also expressed in 1D and 2D NMR spectroscopic studies. With increasing binding affinities of guests toward the receptor, the complexes show slow exchange on the NMR time scale, further enabling characterization of guests in the interior of the host (see Supporting Information, Sections S8 and S9).

At slow exchange on the NMR time scale, formation of diastereoisomeric complexes of enantiopure hosts, $(P)_4$-**1** or $(M)_4$-**1**, with chiral racemic guests results in two diastereoisomeric NMR resonances. The diagnostic splitting of 1D NMR signals−observed in the ^{1}H, ^{13}C, and ^{19}F NMR traces−is comparable to effects observed with chiral shift reagents. They allow identification of the enantioselectivity of enantiopure hosts toward chiral guests in solution (see Supporting Information, Sections S8 and S9). In particular, the splitting of the O*H*-bonding array resonance of the host enables a fast and reliable readout of the enantioselectivities. In addition, the relative occupancy of enantiomers inside the receptor in X-ray cocrystal structures gives insight into enantioselectivities in the

https://dx.doi.org/10.1021/jacs.9b13217
J. Am. Chem. Soc. XXXX, XXX, XXX−XXX

solid state. The enantioselectivities observed in solution match well with the ones observed in the solid state.

In order to demonstrate reliability of the diastereoisomeric readout of host–guest complexes in solution, we separated three of the stronger binding guests, namely (*R**,*S**)-**8**, (*R**,*R**)-**8**, and (*R**,*R**)-**10**, into their respective enantiomers (see Supporting Information, Section S2).

Figure 5A gives a summary of the differences in binding affinities of enantiopure guests with $(P)_4$-configured host **1** and compares those to the diastereoisomeric ratios observed in NMR and X-ray crystallographic analysis.

While the difference in binding affinity of (*S*,*R*)-**8** and (*R*,*S*)-**8** is negligible ($\Delta\Delta G_{293\ K}$ = −0.1 kcal mol^{-1}), inversion of a single stereocenter to (*S*,*S*)-**8** and (*R*,*R*)-**8** results in substantially higher enantioselectivity of $\Delta\Delta G_{293\ K}$ = −0.7 kcal mol^{-1}. ITC results further show that the stronger binding of one enantiomer results in a gain in enthalpy ΔH (−12.3 → −13.3 kcal mol^{-1}), however at the cost of a larger entropic term $T\Delta S$ (+4.8 → +5.2 kcal mol^{-1}; see Tables S32 and S33). This trend is also observed for guest **10**, where enantioselectivities between (*S*,*S*)-**10** and (*R*,*R*)-**10** amount to $\Delta\Delta G_{293\ K}$ = −0.7 kcal mol^{-1} (ΔH = −12.6 → −14.3 kcal mol^{-1}; $T\Delta S$ = +5.0 → +6.0 kcal mol^{-1}; see Tables S36 and S37). This emphasizes that stronger binding, accompanied by gain in enthalpy, comes with an entropic penalty. Figure 5B gives an overlay of ^{1}H NMR spectroscopic traces of $(P)_4$-**1** with racemic (*R**,*R**)-**8** and the stronger binding (*R*,*R*)-**8** enantiomer. Diagnostic splitting of the diastereoisomeric ^{1}H NMR spectroscopic resonances is only observed for the racemic guest compound, allowing for the full characterization of both diastereoisomeric complexes in solution.

Single crystal X-ray structure of $(P)_4$-**1** with both enantiomers of (*R**,*R**)-**8** (Figure 5C) substantiates the difference in binding strength of the enantiomeric pair. The stronger binding (*R*,*R*)-**8** forms a puckered 5-fold H-bonding array with the host. The Br-substituent in the 2-position forms favorable C–Br···π interactions with the aromatic resorcin[4]-arene core (average distances of 4.3 Å), while the second Br is in close contact with the acetylenic moiety (C–Br···||| of 3.3 Å; α_{XB} = 160°). In comparison, the hydroxy group of the weaker binding (*S*,*S*)-**8** forms an energetically less favorable 4-fold and docking topology with the H-bonding array of the host.[4] The Br-substituent in position 2 now forms C–Br···||| contacts of 3.7 Å (α_{XB} = 140°), and the second Br interacts with the aromatic core of the receptor (average distances of C–Br···π of 4.1 Å). These subtle differences in geometry, mainly of the OH-array,[4] of the two enantiomeric complexes result in substantial differences in binding energy between the two enantiomers of $\Delta\Delta G_{293\ K}$ = 0.7 kcal mol^{-1}.

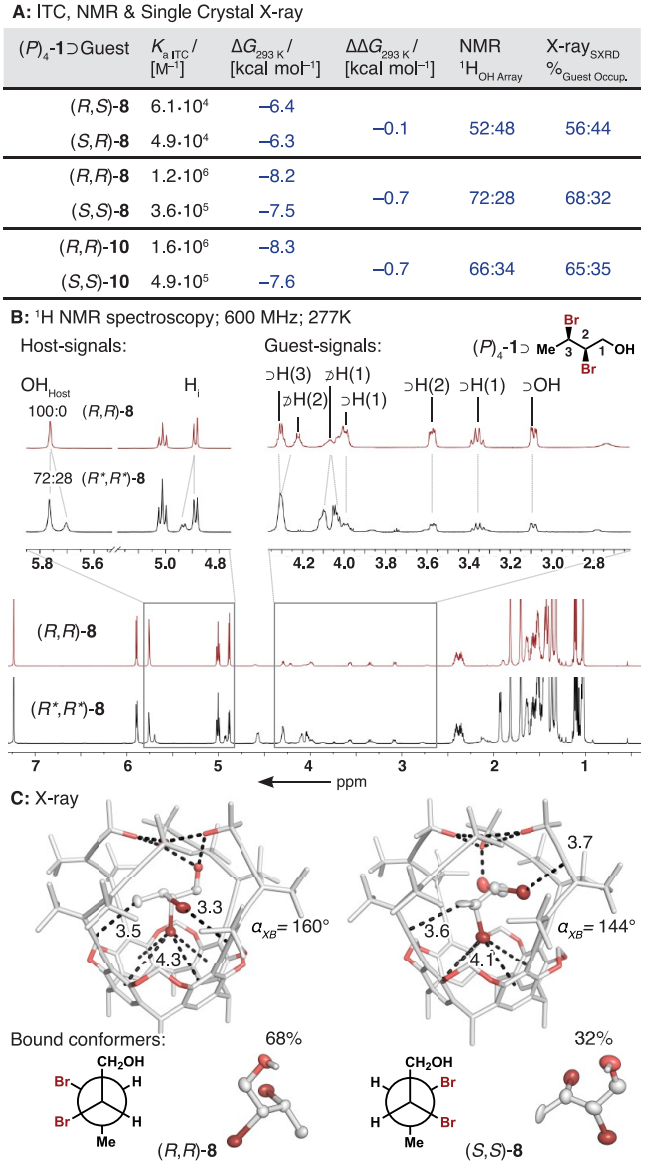

Figure 5. A) Association constants (K_a) and Gibbs binding energies ($\Delta G_{293\ K}$) obtained by ITC for the encapsulation of the enantiopure guests by $(P)_4$-**1**; the overall error in K_a is estimated to be ±20% ($\Delta G_{293\ K}$ ± 0.2 kcal mol^{-1}); diastereoisomeric ratios are given for the $^1H_{OH}$ resonance of the host (600 MHz, at 277 K); relative occupancies of the enantiomeric pairs are derived from the single crystal X-ray structures (error margin of ±5%). B) Overlay of the 600 MHz ^{1}H NMR spectroscopic traces of $(P)_4$-**1** with the enantiopure (*R*,*R*)-**8** (1.5 equiv guest with 1 equiv bound to the host and 0.5 equiv free in solution, top) and the racemic (*R**,*R**)-**8** (3 equiv with 1 equiv bound to the host and 2 equiv free in solution, signals correspond to two sets of diastereoisomers of the host-bound guests and free guest signals, bottom) in *n*-octane-d_{18} at 277 K. C) X-ray cocrystal structures of $(P)_4$-**1** with racemic (*R**,*R**)-**8**. Distances are given in Å. CCDC 1914842.

CONCLUSION

Enantiopure alleno-acetylenic cage receptors $(P)_4$- and $(M)_4$-**1** offer well-defined, mostly lipophilic environments for complexation of fragments of the natural product danicalipin A. Fast readout of complexation in solution and solid state is presented and allows, for the first time, a study of their conformation in a more hydrophobic environment. Functional group replacements on the core chlorohydrin fragment led to a series of 14 molecules with up to two stereogenic centers. The highly retained binding mode of guest structures **7**–**10** in the host interior gives insight into the influence of functional group replacements toward the Gibbs binding energies of the ensemble. Generally, binding strength increases along the series Me → Cl → Br with the establishment and strengthening of halogen-bonding contacts and with reduced conformational energy costs. The *syn*-products (*R**,*R**) bind by $\Delta\Delta G_{293\ K} \approx 1$ kcal mol^{-1} stronger compared to the *anti*-products (*R**,*S**), which is a result of the conformational energies associated with adopting the preferred host-bound *gauche* conformation. The strongest binding affinities are observed for the Br-derivatives (*R**,*R**)-**8** and -**10** with Gibbs

https://dx.doi.org/10.1021/jacs.9b13217
J. Am. Chem. Soc. XXXX, XXX, XXX–XXX

binding energies of $\Delta G_{293\ K} = -7.6$ and -7.5 kcal mol^{-1} (K_d = 2.1 μM and 2.6 μM), respectively. Denser packing and optimized dispersion interactions in inclusion complexes did not lead to higher binding affinities. Remarkably, achiral guest **9** is complexed in two chiral conformations with higher occupancy of one conformational enantiomer, exemplifying the highly asymmetric environment of the interior of the receptor. The enantioselectivities of the enantiopure receptor toward chiral guests were assessed in solution and solid state. The diagnostic splitting of the diastereoisomeric OH-bonding array resonances of the host upon complexation of chiral racemic guests enables fast readout of enantioselectivities. Separation of stronger binding guests into their respective enantiomers demonstrated the reliability of this readout. The X-ray cocrystal structures of $(P)_4$-**1** with (*R*,*R*)-**8** and (*S*,*S*)-**8** (68:32 relative occupancies) reveal subtle differences in hydrogen-bonding, halogen-bonding, and dispersion interactions between the two enantiomers that result in a difference in Gibbs binding energy of up to $\Delta\Delta G_{293\ K} = 0.7$ kcal mol^{-1}. Calorimetric studies (ITC) further show that the stronger binding of one enantiomer is accompanied by an increase in enthalpy ΔH but at the cost of a larger entropic penalty stemming from tighter binding.

This fragment-based complexation study gives first insight into preferred conformations of methylated and halogenated structures in a more hydrophobic environment[2b] and complements the extensive conformational analysis studies of the free fragments in polar solvents. Importantly, the AAC model system exposes the influence of conformational energies and preorganization toward binding affinities and allows drawing the conclusion that denser packing of apolar side chains in the complex does not necessarily result in higher association. Finally, we wish to point out that this is one of the first detailed host–guest complexation studies with neutral receptors and neutral small acyclic guests.

■ ASSOCIATED CONTENT

Supporting Information

The Supporting Information is available free of charge at https://pubs.acs.org/doi/10.1021/jacs.9b13217.

CCDC 1914836, 1914837, 1914838, 1914839, 1914840, 1914841, 1914842, 1914843, 1914852, 1914853, 1914854, 1914855, 1914856, 1914857, 1914858, 1914859 (AAC $(P)_4$- and $(M)_4$-**1** ⊃Guest) contain supplementary crystallographic data (ZIP)

Optimized structures and single point energies obtained from the theoretical studies attached as xyz files (ZIP)

Detailed synthetic procedures and separation methods of guests molecules; binding experiments with binding isotherms, association constants (K_a) by ECD spectroscopy and ITC; guest complexation studies by 1D and 2D NMR spectroscopy; *J*-based conformation analysis; single crystal X-ray structures; NMR spectra of AACs and guests compounds; computational methodology; conformational analysis of alcohols **2**–**12** in gas and condensed phase; effect of computational methodology; packing coefficients of host–guest complexes (PDF)

■ AUTHOR INFORMATION

Corresponding Authors

Erick M. Carreira − *Laboratorium für Organische Chemie, ETH Zurich, CH-8093 Zurich, Switzerland;* orcid.org/0000-0003-1472-490X; Email: carreira@org.chem.ethz.ch

François Diederich − *Laboratorium für Organische Chemie, ETH Zurich, CH-8093 Zurich, Switzerland;* orcid.org/0000-0003-1947-6327; Email: diederich@org.chem.ethz.ch

Authors

Cornelius Gropp − *Laboratorium für Organische Chemie, ETH Zurich, CH-8093 Zurich, Switzerland*

Stefan Fischer − *Laboratorium für Organische Chemie, ETH Zurich, CH-8093 Zurich, Switzerland*

Tamara Husch − *Laboratorium für Physikalische Chemie, ETH Zurich, CH-8093 Zurich, Switzerland; Division of Chemistry and Chemical Engineering, California Institute of Technology, Pasadena, California 91125, United States;* orcid.org/0000-0002-2880-2481

Nils Trapp − *Laboratorium für Organische Chemie, ETH Zurich, CH-8093 Zurich, Switzerland*

Complete contact information is available at: https://pubs.acs.org/10.1021/jacs.9b13217

Funding

C.G. was supported by the Studienstiftung des Deutschen Volkes. We are grateful for the support by the ETH Research Council (ETH-01 13-2) and the Swiss National Science Foundation (SNF 200020_159802).

Notes

The authors declare no competing financial interest.

CCDC data can be obtained free of charge from The Cambridge Crystallographic Data Centre.

■ ACKNOWLEDGMENTS

We thank René Arnold and Rainer Frankenstein for recording NMR spectra, Michael Solar for recording single-crystal X-ray structures, and Dr. Anatol Schwab for valuable comments on the manuscript.

■ REFERENCES

(1) (a) *Inclusion Compounds*, Atwood, J. L., Davies, J. E. D., MacNicol, D. D., Eds.; Academic Press: London, 1984. (b) Dunitz, J. D. *X-ray Analysis and the Structure of Organic Molecules*; Cornell University Press: Ithaca, 1995; DOI: 10.1002/9783906390390. (c) Rebek, J., Jr. Molecular Behavior in Small Spaces. *Acc. Chem. Res.* **2009**, *42*, 1660–1668. (d) Legrand, Y.-M.; van der Lee, A.; Barboiu, M. Single-Crystal X-ray Structure of 1,3-Dimethylcyclobutadiene by Confinement in a Crystalline Matrix. *Science* **2010**, *329*, 299–302. (e) Inokuma, Y.; Yoshioka, S.; Ariyoshi, J.; Arai, T.; Hitora, Y.; Takada, K.; Matsunaga, S.; Rissanen, K.; Fujita, M. X-ray Analysis on the Nanogram to Microgram Scale Using Porous Complexes. *Nature* **2013**, *495*, 461–466. (f) Matsuzaki, S.; Arai, T.; Ikemoto, K.; Inokuma, Y.; Fujita, M. Networked-Cage Microcrystals for Evaluation of Host–Guest Interactions. *J. Am. Chem. Soc.* **2014**, *136*, 17899–17901. (g) Catti, L.; Zhang, Q.; Tiefenbacher, K. Advantages of Catalysis in Self-Assembled Molecular Capsules. *Chem. - Eur. J.* **2016**, *22*, 9060–9066. (h) Lee, S.; Kapustin, E. A.; Yaghi, O. M. Coordinative Alignment of Molecules in Chiral Metal-Organic Frameworks. *Science* **2016**, *353*, 808–811. (i) Rissanen, K. Crystallography of Encapsulated Molecules. *Chem. Soc. Rev.* **2017**, *46*, 2638–2648. (j) Rizzuto, F. J.; Carpenter, J. P.; Nitschke, J. R. Multisite Binding of Drugs and Natural Products in an Entropically Favorable, Heteroleptic Receptor. *J. Am. Chem. Soc.* **2019**, *141*, 9087–

9095. (k) Takezawa, H.; Kanda, T.; Nanjo, H.; Fujita, M. Site-Selective Functionalization of Linear Diterpenoids through U-Shaped Folding in a Confined Artificial Cavity. *J. Am. Chem. Soc.* **2019**, *141*, 5112−5115.

(2) (a) Gropp, C.; Trapp, N.; Diederich, F. Alleno-Acetylenic Cage (AAC) Receptors: Chiroptical Switching and Enantioselective Complexation of *trans*-1,2-Dimethylcyclohexane in a Diaxial Conformation. *Angew. Chem., Int. Ed.* **2016**, *55*, 14444−14449. (b) Gropp, C.; Husch, T.; Trapp, N.; Reiher, M.; Diederich, F. Dispersion and Halogen-Bonding Interactions: Binding of the Axial Conformers of Monohalo- and (±)-*trans*-1,2-Dihalocyclohexanes in Enantiopure Alleno-Acetylenic Cages. *J. Am. Chem. Soc.* **2017**, *139*, 12190−12200. (c) Gropp, C.; Quigley, B. L.; Diederich, F. Molecular Recognition with Resorcin[4]arene Cavitands: Switching, Halogen-Bonded Capsules, and Enantioselective Complexation. *J. Am. Chem. Soc.* **2018**, *140*, 2705−2717. (d) Gropp, C.; Trapp, N. Complexation and Structure Elucidation of the Axial Conformers of Mono- and (±)-*trans*-1,2-Disubstituted Cyclohexanes by Enantiopure Alleno-Acetylenic Cage Receptors. *Chimia* **2018**, *72*, 245−248.

(3) Caprice, K.; Pupier, M.; Bauzá, A.; Frontera, A.; Cougnon, F. B. L. Synchronized On/Off Switching of Four Binding Sites for Water in a Molecular Solomon Link. *Angew. Chem., Int. Ed.* **2019**, *58*, 8053−8057.

(4) Gropp, C.; Husch, T.; Trapp, N.; Reiher, M.; Diederich, F. Hydrogen-Bonded Networks: Molecular Recognition of Cyclic Alcohols in Enantiopure Alleno-Acetylenic Cage Receptors. *Angew. Chem., Int. Ed.* **2018**, *57*, 16296−16301.

(5) Schneider, H.-J. Dispersive Interactions in Solution Complexes. *Acc. Chem. Res.* **2015**, *48*, 1815−1822.

(6) (a) Haines, T. H.; Pousada, M.; Stern, B.; Mayers, G. L. Microbial Sulpholipids: (*R*)-13-Chloro-1-(*R*)-14-docosanediol Disulphate and Polychlorosulpholipids in Ochromonas Danica. *Biochem. J.* **1969**, *113*, 565−566. (b) Elovson, J.; Vagelos, P. R. A New Class of Lipids: Chlorosulfolipids. *Proc. Natl. Acad. Sci. U. S. A.* **1969**, *62*, 957−963. (c) Nilewski, C.; Geisser, R. W.; Carreira, E. M. Total Synthesis of a Chlorosulpholipid Cytotoxin Associated with Seafood Poisoning. *Nature* **2009**, *457*, 573−577. (d) Bedke, D. K.; Vanderwal, C. D. Chlorosulfolipids: Structure, Synthesis, and Biological Relevance. *Nat. Prod. Rep.* **2011**, *28*, 15−25. (e) Nilewski, C.; Carreira, E. M. Recent Advances in the Total Synthesis of Chlorosulfolipids. *Eur. J. Org. Chem.* **2012**, *2012*, 1685−1698. (f) Sondermann, P.; Carreira, E. M. Stereochemical Revision, Total Synthesis, and Solution State Conformation of the Complex Chlorosulfolipid Mytilipin B. *J. Am. Chem. Soc.* **2019**, *141*, 10510−10519.

(7) (a) Bailey, A. M.; Wolfrum, S.; Carreira, E. M. Biological Investigations of (+)-Danicalipin A Enabled Through Synthesis. *Angew. Chem., Int. Ed.* **2016**, *55*, 639−643. (b) Fischer, S.; Huwyler, N.; Wolfrum, S.; Carreira, E. M. Synthesis and Biological Evaluation of Bromo- and Fluorodanicalipin A. *Angew. Chem., Int. Ed.* **2016**, *55*, 2555−2558. (c) Boshkow, J.; Fischer, S.; Bailey, A. M.; Wolfrum, S.; Carreira, E. M. Stereochemistry and Biological Activity of Chlorinated Lipids: A Study of Danicalipin A and Selected Diastereomers. *Chem. Sci.* **2017**, *8*, 6904−6910.

(8) Nilewski, C.; Geisser, R. W.; Ebert, M.-O.; Carreira, E. M. Conformational and Configurational Analysis in the Study and Synthesis of Chlorinated Natural Products. *J. Am. Chem. Soc.* **2009**, *131*, 15866−15876.

(9) (a) Zürcher, M.; Diederich, F. Structure-Based Drug Design: Exploring the Proper Filling of Apolar Pockets at Enzyme Active Sites. *J. Org. Chem.* **2008**, *73*, 4345−4361. (b) Mravic, M.; Thomaston, J. L.; Tucker, M.; Solomon, P. E.; Liu, L.; DeGrado, W. F. Packing of Apolar Side Chains Enables Accurate Design of Highly Stable Membrane Proteins. *Science* **2019**, *363*, 1418−1423.

(10) (a) Meanwell, N. A. Synopsis of Some Recent Tactical Application of Bioisosteres in Drug Design. *J. Med. Chem.* **2011**, *54*, 2529−2591. (b) Krautwald, S.; Nilewski, C.; Mori, M.; Shiomi, K.; Ōmura, S.; Carreira, E. M. Bioisosteric Exchange of C_{sp3}-Chloro and Methyl Substituents: Synthesis and Initial Biological Studies of Atpenin A5 Analogues. *Angew. Chem., Int. Ed.* **2016**, *55*, 4049−4053.

(11) Biedermann, F.; Schneider, H.-J. Experimental Binding Energies in Supramolecular Complexes. *Chem. Rev.* **2016**, *116*, 5216−5300.

(12) CCDC 1914836, 1914837, 1914838, 1914839, 1914840, 1914841, 1914842, 1914843, 1914852, 1914853, 1914854, 1914855, 1914857, 1914858, 1914859 (AAC $(P)_4$- and $(M)_4$-**1** ⊃Guest) contain the supplementary crystallographic data for this paper. These data can be obtained free of charge from The Cambridge Crystallographic Data Centre.

(13) (a) Perdew, J. P.; Wang, Y. Accurate and Simple Analytic Representation of the Electron-gas Correlation Energy. *Phys. Rev. B: Condens. Matter Mater. Phys.* **1992**, *45*, 13244−13249. (b) Perdew, J. P.; Burke, K.; Ernzerhof, M. Generalized Gradient Approximation Made Simple. *Phys. Rev. Lett.* **1996**, *77*, 3865−3868.

(14) Grimme, S.; Antony, J.; Ehrlich, S.; Krieg, H. A Consistent and Accurate Ab Initio Parametrization of Density Functional Dispersion Correction (DFT-D) for the 94 Elements H-Pu. *J. Chem. Phys.* **2010**, *132*, 154104.

(15) Weigend, F.; Ahlrichs, R. Balanced Basis Sets of Split Valence, Triple Zeta Valence and Quadruple Zeta Valence Quality for H to Rn: Design and Assessment of Accuracy. *Phys. Chem. Chem. Phys.* **2005**, *7*, 3297−3305.

(16) (a) Swierczynski, D.; Luboradzki, R.; Dolgonos, G.; Lipkowski, J.; Schneider, H.-J. Non-Covalent Interactions of Organic Halogen Compounds with Aromatic Systems − Analyses of Crystal Structure Data. *Eur. J. Org. Chem.* **2005**, *2005*, 1172−1177. (b) Salonen, L. M.; Ellermann, M.; Diederich, F. Aromatic Rings in Chemical and Biological Recognition: Energetics and Structures. *Angew. Chem., Int. Ed.* **2011**, *50*, 4808−4842.

(17) (a) Rivera, J. M.; Martin, T.; Rebek, J., Jr. Chiral Spaces: Dissymmetric Capsules through Self-Assembly. *Science* **1998**, *279*, 1021−1023. (b) Rivera, J. M.; Rebek, J., Jr. Chiral Space in a Unimolecular Capsule. *J. Am. Chem. Soc.* **2000**, *122*, 7811−7812. (c) Scarso, A.; Shivanyuk, A.; Hayashida, O.; Rebek, J., Jr. Asymmetric Environments in Encapsulation Complexes. *J. Am. Chem. Soc.* **2003**, *125*, 6239−6243.

(18) Ajami, D.; Rebek, J., Jr Compressed Alkanes in Reversible Encapsulation Complexes. *Nat. Chem.* **2009**, *1*, 87−90.

(19) Müller, K.; Faeh, C.; Diederich, F. Fluorine in Pharmaceuticals: Looking Beyond Intuition. *Science* **2007**, *317*, 1881−1886.

(20) (a) Metrangolo, P.; Meyer, F.; Pilati, T.; Resnati, G.; Terraneo, G. Halogen Bonding in Supramolecular Chemistry. *Angew. Chem., Int. Ed.* **2008**, *47*, 6114−6127. (b) Dumele, O.; Trapp, N.; Diederich, F. Halogen Bonding Molecular Capsules. *Angew. Chem., Int. Ed.* **2015**, *54*, 12339−12344. (c) Persch, E.; Dumele, O.; Diederich, F. Molecular Recognition in Chemical and Biological Systems. *Angew. Chem., Int. Ed.* **2015**, *54*, 3290−3327. (d) Cavallo, G.; Metrangolo, P.; Milani, R.; Pilati, T.; Priimagi, A.; Resnati, G.; Terraneo, G. The Halogen Bond. *Chem. Rev.* **2016**, *116*, 2478−2601.

(21) Mecozzi, S.; Rebek, J., Jr. The 55% Solution: A Formula for Molecular Recognition in the Liquid State. *Chem. - Eur. J.* **1998**, *4*, 1016−1022.

https://dx.doi.org/10.1021/jacs.9b13217
J. Am. Chem. Soc. XXXX, XXX, XXX−XXX